Nearby Supernova Factory Observations of SN 2006D: On Sporadic Carbon Signatures in Early Type Ia Supernova Spectra

The Nearby Supernova Factory

R. C. Thomas,[1] G. Aldering,[1] P. Antilogus,[3] C. Aragon,[1] S. Bailey,[1] C. Baltay,[8] E. Baron,[9] A. Bauer,[8] C. Buton,[2] S. Bongard,[1,5] Y. Copin,[2] E. Gangler,[2] S. Gilles,[3] R. Kessler,[7] S. Loken,[1] P. Nugent,[1] R. Pain,[3] J. Parrent,[9] E. Pécontal,[4] R. Pereira,[3] S. Perlmutter,[1,6] D. Rabinowitz,[8] G. Rigaudier,[4] K. Runge,[1] R. Scalzo,[1] G. Smadja,[2] L. Wang,[1] B. A. Weaver[1,5]

Received _____; accepted _____

To appear in Astrophysical Journal Letters

[1]Physics Division, Lawrence Berkeley National Laboratory, 1 Cyclotron Road, Berkeley, CA 94720

[2]Institut de Physique Nucléaire de Lyon, UMR5822, CNRS-IN2P3; Université Claude Bernard Lyon 1, F-69622 Villeurbanne France

[3]Laboratoire de Physique Nucléaire et des Hautes Energies IN2P3 - CNRS - Universités Paris VI et Paris VII, 4 place Jussieu Tour 33 - Rez de chaussée 75252 Paris Cedex 05

[4]Centre de Recherche Astronomique de Lyon, 9, av. Charles André, 69561 Saint Genis Laval Cedex

[5]University of California, Space Sciences Laboratory, Berkeley, CA 94720-7450

[6]Department of Physics, University of California, Berkeley, CA 94720

[7]Kavli Institute for Cosmological Physics, The University of Chicago, Chicago, IL 60637

[8]Department of Physics, Yale University, New Haven, CT 06250-8121

[9]Homer L. Dodge Department of Physics and Astronomy, 440 W. Brooks Street, University of Oklahoma, Norman, OK 73019

ABSTRACT

We present four spectra of the Type Ia supernova (SN Ia) 2006D extending from −7 to +13 days with respect to B-band maximum. The spectra include the strongest signature of unburned material at photospheric velocities observed in a SN Ia to date. The earliest spectrum exhibits C II absorption features below 14,000 km s^{-1}, including a distinctive C II λ6580 absorption feature. The carbon signatures dissipate as the SN approaches peak brightness. In addition to discussing implications of photospheric-velocity carbon for white dwarf explosion models, we outline some factors that may influence the frequency of its detection before and around peak brightness. Two effects are explored in this regard, including depopulation of the C II optical levels by non-LTE effects, and line-of-sight effects resulting from a clumpy distribution of unburned material with low volume-filling factor.

Subject headings: supernovae: general — supernovae: individual (SN 2006D)

1. Introduction

Type Ia supernovae (SNe Ia) make valuable standard candles because of their intrinsic brightness and the homogeneity of their light curves. Observations of high-redshift SNe Ia are responsible for the recent revelation that the rate of expansion of the Universe is accelerating (Perlmutter et al. 1998; Garnavich et al. 1998; Riess et al. 1998; Perlmutter et al. 1999). A push to better calibrate SNe Ia as distance indicators and control systematics in future high-precision cosmology experiments has helped motivate the search for deeper physical insight into SN Ia progenitors and their explosion mechanism.

Certain recent multidimensional hydrodynamical SN Ia explosion models involve the thermonuclear disruption of a Chandrasekhar-mass C-O white dwarf (WD) by *deflagration*, the propagation of a subsonic flame front through the star (e.g., Gamezo et al. 2003; Röpke & Hillebrandt 2005). A generic characteristic of these new models is the presence of unprocessed WD material below the canonical 14,000 km s^{-1} cutoff seen in W7, a tuned spherically-symmetric deflagration model (Nomoto, Thielemann & Yokoi 1984). Thus, carbon detection at such low velocities would provide observational support for the newer multidimensional deflagration models. Few SN Ia spectra actually exhibit a robust low-velocity carbon signature; to date the lowest measured are the C II λ6580 and λ7234 features in the spectra of SN 1998aq, which may extend deeper than 11,000 km s^{-1} (Branch et al. 2003). The lack of ubiquitous carbon signatures in the spectra of SNe Ia, and the observed deficit of kinetic energy and synthesized nickel indicate that these models are not viable, though increasingly sophisticated models (e.g., with greater resolution and more detailed nucleosynthesis) may prove otherwise. Most recently, Marion et al. (2006) used near-infrared spectroscopy to conclude that nuclear burning in at least three normal SNe Ia is complete below 18,000 km s^{-1}, a conclusion supporting models where an initial deflagration transitions to a supersonic *detonation* (Khokhlov 1991).

We present Nearby Supernova Factory (SNfactory, Aldering et al. 2002) spectroscopy of the SN Ia 2006D, which includes an unambiguous photospheric-velocity C II signature. The data were obtained using the Supernova Integral Field Spectrograph (SNIFS, Aldering et al. 2002; Lantz et al. 2004) on the University of Hawaii 2.2-meter telescope on Mauna Kea. Our focus here is on the early photospheric-phase spectra of SN 2006D; an analysis involving all of our data will appear elsewhere.

2. Data & Analysis

The Brazilian Supernova Search (Colesanti et al. 2006) discovered SN 2006D in MCG -01-33-34 ($z = 0.00853$, Davoust & Contini 2004) on 2006 January 11.2 UTC. Using a SNIFS spectrum obtained January 14.6 UTC, we classified SN 2006D as a SN Ia one week prior to maximum brightness (SNfactory 2006). This and three subsequent spectra appear in Figure 1 and are summarized in Table 1. The spectra were reduced using our dedicated data-reduction procedure, similar to that presented in § 4 of Bacon et al. (2001) and § 2 of Aldering et al. (2006). No correction for interstellar reddening has been applied. The intermediate-mass element (IME) spectral features typical of premaximum SNe Ia are labelled on the first spectrum for reference. A preliminary light curve fit derived from SNIFS acquisition images indicates a B-band peak date of 2006 January 21.8 UTC, and a stretch parameter $s \sim 0.75$, significantly lower than that of a typical "normal" SN Ia ($s \equiv 1$). This value is similar to that derived from the light curves of SNe 1986G and 1992bo (0.74 and 0.73 respectively, Guy et al. 2005), but not as extreme as in the subluminous SNe 1991bg or 1999by ($s \sim 0.6$; Ruiz-Lapuente 2004; Garnavich et al. 2004; Jha 2006).

The dotted vertical lines in Figure 1 indicate the rest-frame wavelengths of the four C II lines that would be the strongest under the assumption of local thermodynamic equilibrium (LTE) at 10,000 K. The shaded regions to the blue of each line cover Doppler

shifts between 14,000 and 10,000 km s^{-1}, representing velocities typical of the photosphere before and around peak brightness. A striking feature of the −7 day spectrum is the ∨-shaped absorption centered at 6320 Å (rest frame), which we attribute to C II λ6580 at a Doppler shift of 12,000 km s^{-1}. In the first spectrum, two much weaker notches fall within the bands of the shaded regions corresponding to C II $\lambda\lambda$4745 and 7234. These two features and the 6580 Å notch weaken by day +13.

Another interesting feature in our spectra is the notch centered at 4100 Å, just to the red of the small absorption typically attributed to Si II $\lambda\lambda$4128,4131. If the 4100 Å absorption is due to C II λ4267, then it extends from 14,000 km s^{-1} down to 8,000 km s^{-1}, slower than the red edge of the λ6580 absorption by 2,000 km s^{-1} (of course, such a low velocity edge could be the result of line-blending). While the other C II features dissipate by day +13, the 4100 Å notch persists and the absorption along its red edge strengthens somewhat. In later spectra not shown here, this feature steadily becomes washed out by iron peak lines in this part of the spectrum. If this feature does arise from C II λ4267, then it does so nonthermally — in LTE at 10,000 K it would be approximately 30 times weaker than C II λ6580; we return to this point shortly.

In Figure 2, we plot our earliest spectrum together with premaximum spectra of SNe 1998aq, 1986G, and 1999by. The spectrum of SN 1998aq is an excellent match to that of SN 2006D, particularly redward of 4400 Å, aside from the stronger C II λ6580 absorption in the latter. Blueward of 4400 Å, the agreement is not as good; the 4100 Å notch in the spectrum of SN 2006D has no counterpart in that of SN 1998aq save for a minor wiggle (in fact, this wiggle has been previously observed in the spectra of SNe Ia, see Figure 2 of Branch et al. 2006). The spectra of SNe 1986G and 1999by exhibit larger Si II 5800 Å to Si II 6150 Å absorption ratios than does SN 2006D, indicative of lower temperature than in more spectroscopically normal SNe Ia (Nugent et al. 1995). The region from 4000 to

4400 Å in these two spectra is dominated by Ti II, also characteristic of lower temperature. The differences between the spectra of SN 2006D and SN 1998aq in this region and the low stretch parameter derived for SN 2006D suggest that Ti II may play a role in the formation of its spectrum.

More detailed SN spectral line identification requires an accounting for line blending, so we compare the −7 day spectrum of SN 2006D with spectra generated by the highly-parameterized SN spectrum synthesis code SYNOW (e.g., Branch et al. 2003). SYNOW uses a simplified model of a SN atmosphere consisting of a sharply-defined continuum-emitting core surrounded by a line-forming region. Line formation is treated under the Sobolev approximation, with line opacity parameterized as a function of ejection velocity and with relative strengths for a given ion set by assuming Boltzmann-factor population of the levels. A synthetic spectrum is overlaid on the observed −7 day spectrum in Figure 3.

The dashed fit reproduces most of the main absorption features of the spectrum, including those of IME ions Ca II, Si II, and S II. A velocity at the photosphere of 11,000 km s^{-1} produces satisfactory results. The blend at 4700 Å consists of lines of Fe II and Si II, while the blend from 4100 Å to 4400 Å consists of lines from Fe III, Mg II, and Si III, and indeed some Ti II (which also fits the absorption at 3600 Å as well). This Ti II detection is consistent with cooler, low-stretch SNe Ia.

The sharpness of the λ6320 feature, and the lack of a discernable accompanying emission feature to its red would suggest that the C II lines are forming in either a layer "detached" from the photosphere (Jeffery & Branch 1990), or in a clump partially obscuring the photosphere along the line of sight (Thomas et al. 2002). The feature seems inconsistent with a thin shell of opacity immediately above the photosphere — such a case would result in a flat trough instead of a sharp downward spike. In the synthetic spectrum, C II opacity

is detached from the photosphere to a velocity of 12,000 km s^{-1}, producing a good match to the C II $\lambda\lambda$6350 and 7234 features. The dotted synthetic spectra in the insets of Figure 3 are from a pure C II spectrum, overlaid on the neighborhoods of the observed C II $\lambda\lambda$4745, 6580, and 7234 features.

We can account for the 4100 Å feature with a separate higher velocity Ti II component (included in the fit with $v > 17,000$ km s^{-1}) but ultimately reject this hypothesis due to the lack of any sign of high-velocity components to explain other spectral features. In particular, Ca II opacity should trace the same high-velocity processed material, and we detect no such signature.

In the absence of any obvious alternative to Ti II for the 4100 Å notch, we suggest that the feature could come from C II λ4267, stimulated by some non-LTE process. To investigate this hypothesis, we examined the non-LTE departure coefficients ($b_i \equiv n_i/n_i^{LTE}$, where n_i is the population number of the atomic level, i) of the lower levels of the optical C II lines in a `PHOENIX` calculation of the model W7 (Baron et al. 2006). In the C-O-rich zone, departure coefficients in optical lines are found to be significantly smaller than unity (10^{-7} to 10^{-3}). Furthermore, the ratio of the λ4267 lower-level b_i to that of λ6580 is observed to range between 1 and 60. This situation arises due to more efficient recombination through the ultraviolet resonance line C II λ687, so that recombination into the optical levels is suppressed and they take on level populations significantly smaller than LTE. The size of this ratio could account for the persistence of C II λ4267 while the other C II lines dissipate. Further detailed models are required to discover whether this effect is indeed generic and holds in other models besides W7. This effect may also resolve the long-standing difficulty of making a reliable identification of C II in the spectra of SNe Ia.

3. Discussion

That some SN Ia spectra possess carbon signatures, particularly before maximum light, is now quite clear. Past tentative identifications of C II λ6580 in such cases as SN 1990N (Mazzali 2001) and SN 1999ac (Garavini et al. 2005), and previously unidentified notches seen in SN 1994D and SN 1996X pointed out by Branch et al. (2003) now seem more meaningful. These detections and their circumstances prompt consideration of several issues relevant to the study of SN Ia explosion models.

The primary issue is the amount of carbon detected. To place a lower limit on the carbon mass (particularly in light of the small b_i's observed in the PHOENIX model), we compute LTE electron level populations and corresponding C II λ6580 Sobolev optical depth on a temperature-density grid, assuming a C-O-rich composition. The absolute minimum density giving rise to optical depth $\tau \sim 1$ at 10 days after outburst is 5.9×10^{-15} g cm^{-3}. Treating this as an average density results in a lower limit of 0.007 $M_\odot$ of carbon (0.014 $M_\odot$ of unburned material) over the velocity range 10,000 to 14,000 km s^{-1} where the absorption feature is detected. This value is smaller than the 0.085 $M_\odot$ of unburned material present at the same velocity interval in the multidimensional model *b150_3d* of Röpke et al. (2006).

If the behavior of the C II b_i's seen in the C-O-rich zone of the W7 PHOENIX model is generic, then the amount of unburned material detected could be *significantly higher* than this estimate. The b_i's need not be so miniscule as observed in the PHOENIX model — here only a factor of 6 is needed to produce general agreement with model *b150_3d*. Extremely small departure coefficients drive the mass up but the mass is obviously limited by the mass-energy budget of the progenitor, fixed by the Chandrasekhar mass. One clear way to make the detection consistent with this constraint is for the unburned material to be distributed in clumps if the b_i's are indeed very small.

The presence of unburned material at the observed velocities is certainly more consistent

with published multidimensional deflagration models than with delayed-detonation models, where no carbon signature is expected at the velocities observed here. Gamezo, Khokhlov & Oran (2004) do outline a scenario in which a small amount of unburned material in pockets could be left by a delayed detonation — as the detonation wave processes material left between plumes generated during the deflagration phase, abrupt twists and turns could cut it off from fresh WD fuel. Elucidating the details (the mass and spatial distribution of such pockets) will rely on progress in future multidimensional delayed-detonation models.

It is interesting to consider the significance of the sporadic and diverse nature of the detections of the C II λ6580 feature itself. The premaximum rest-frame 5800-6600 Å spectra of SN 2006D and five other SNe Ia plotted in Figure 4 exhibit a variety of strengths and velocity ranges in C II λ6580. The theoretical multidimensional models themselves may suggest an explanation for this phenomenon beyond any non-LTE effect — the distribution of unburned material at these velocities could be quite asymmetric, confined to clumps of small filling factor compared to the photosphere. Thus, differences from SN to SN would naturally be explained as a function of the distribution of the clumps with respect to the observer's line of sight. This argument is consistent with the complementary finding by Thomas et al. (2002), where the relatively consistent shape and depth of Si II λ6355 absorption at maximum light indicates that the distribution of IME's in SNe Ia cannot be highly asymmetric.

4. Conclusions

We have presented the strongest evidence to date of unburned ejecta at low velocity in the early spectra of a SN Ia. The case of SN 2006D reiterates the importance of early-time spectroscopy (and spectropolarimetry) for SN Ia research. Complimentary observations in the nebular phase (one year after explosion) may present further opportunities to probe

the distribution and amount of unburned material at low velocity in SN 2006D; while their predictions are not strictly applicable at the velocities considered in this work, the multidimensional spectrum synthesis models of Kozma et al. (2005) suggest that unburned material at velocities below 10,000 km s^{-1} roughly consistent with our mass estimates may be detectable at late times as forbidden [O I] and [C I] emission.

We are grateful to the technical and scientific staff of the University of Hawaii 2.2-meter telescope for their assistance in obtaining these data. The authors wish to recognize and acknowledge the very significant cultural role and reverence that the summit of Mauna Kea has always had within the indigenous Hawaiian community. We are most fortunate to have the opportunity to conduct observations from this mountain. We also thank F. Röpke for kindly providing the angle-averaged mass distribution of model *b150_3d*. Our analysis included data from the University of Oklahoma Online SUpernova SPECTrum (SUSPECT) Archive. This work was supported in part by the Director, Office of Science, Office of High Energy and Nuclear Physics, of the U.S. Department of Energy under Contract No. DE-FG02-92ER40704, by a grant from the Gordon & Betty Moore Foundation, by National Science Foundation Grant Number AST-0407297, and in France by support from CNRS/IN2P3, CNRS/INSU and PNC. This research used resources of the National Energy Research Scientific Computing Center, which is supported by the Office of Science of the U.S. Department of Energy under Contract No. DE-AC02-05CH11231. We also acknowledge support from the U.S. Department of Energy Scientific Discovery through Advanced Computing program under Contract No. DE-FG02-06ER06-04.

Facilities: UH:2.2m (SNIFS)

REFERENCES

Aldering, G., et al. 2002, Proc. SPIE, 4836, 61

Aldering, G., et al. 2006, ApJ, 650, 510

Bacon, R., et al. 2001, MNRAS, 326, 23

Baron, E., Bongard, S., Branch., D. & Hauschildt, P. 2006, ApJ, 645, 480

Branch, D., et al. 2003, AJ, 126, 1489

Branch, D., et al. 2006, PASP, 118, 560

Colesanti, C., et al. 2006, IAU Circ., 8658, 2

Davoust, E. & Contini, T. 2004, A&A, 416, 515

Gamezo, V., Khokhlov, A. M., Oran, E. S., Chtchelkanova, A., & Rosenberg, R. 2003, Science, 299, 77

Gamezo, V. N., Khokhlov, A. M., & Oran, E. S. 2004, Phys. Rev. Lett., 92, 1102

Garavini, G., et. al. 2005, AJ, 130, 2287

Garnavich, P. M., et al. 1998, ApJ, 493, L53

Garnavich, P. M., et al. 2004, ApJ, 613, 1120

Guy, J., Astier, P., Nobili, S., Regnault, N., & Pain, R. 2005, A&A, 443, 781

Jeffery, D. J. & Branch, D. 1990, Jerusalem Winter School for Theoretical Physics, Vol. 6, ed. J. C. Wheeler & S. Weinberg (Singapore: World Scientific), 149

Jha, S., et al. 2006, AJ, 132, 189

Khokhlov, A. 1991, ApJ, 245, 114

Kozma, C., et al. 2005, A&A, 437, 983

Lantz, B., et al. 2004, Proc. SPIE, 5249, 146

Marion, G. H., et al. 2006, ApJ, 645, 1392

Mazzali, P. A. 2001, MNRAS, 321, 341

Nomoto, K., Thielemman, F.-K., & Yokoi, K. 1984, ApJ, 286, 644

Nugent, P., et al. 1995, ApJ, 455, 147

Perlmutter, S., et al. 1998, Nature, 391, 51

Perlmutter, S., et al. 1999, ApJ, 517, 565

Riess, A. G., et al. 1998, AJ, 116, 1009

Röpke, F. K. & Hillebrandt, W. 2005, A&A, 431, 635

Röpke, F. K., Hillebrandt, W., Niemeyer, J. C., & Woosley, S. E. 2006, A&A, 448, 1

Ruiz-Lapuente, P. 2004, ApJ, 612, 357

The Nearby Supernova Factory 2006, ATel, 689, 1

Thomas, R. C., Kasen, D., Branch, D., Baron, E. 2002, ApJ, 567, 1037

Table 1. Journal of Spectroscopy of SN 2006D

Julian Day	UTC Date (2006)	Exposure (s)	Airmass	Median S/N[a] blue	red	Conditions
2453750.10	Jan. 14.60	900	1.20	76	85	non-photometric
2453752.12	Jan. 16.62	1000	1.16	72	69	cloudy
2453756.07	Jan. 20.57	1800	1.22	205	136	near Moon
2453770.11	Feb. 03.61	1000	1.16	72	93	photometric

[a]Blue channel: 3500-5050 Å with 2.4 Å bins. Red channel: 5000-9000 Å with 3.0 Å bins.

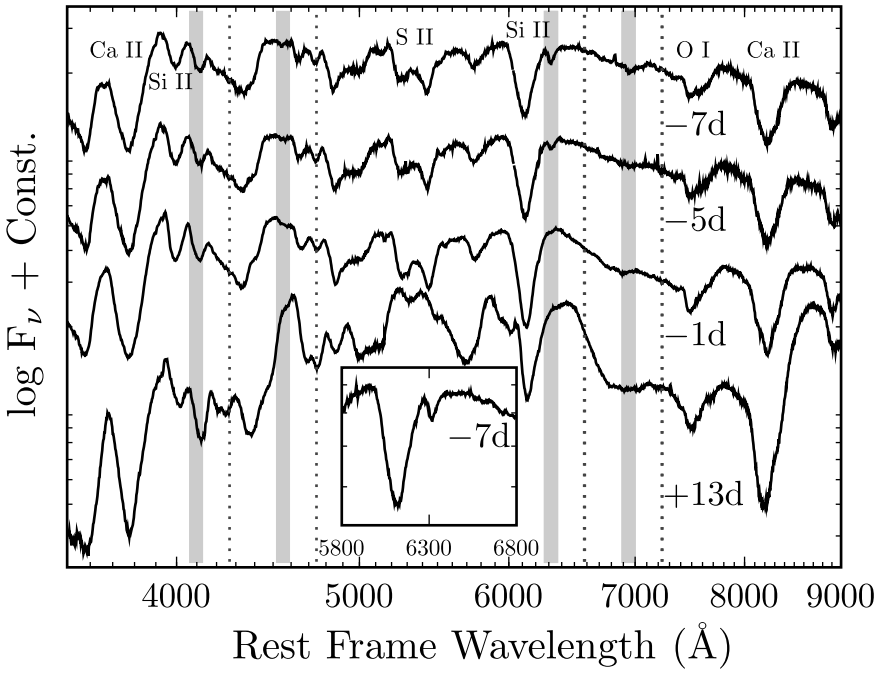

Fig. 1.— SNIFS spectroscopy of SN 2006D. Phases are expressed relative to a B-band peak brightness date of 2006 January 21.8 UTC. Dotted vertical lines mark rest wavelengths of C II lines $\lambda\lambda$4267, 4745, 6580, and 7234. Dark bands indicate blueshifts between 10,000 and 14,000 km s^{-1} with respect to these lines, typical of the velocity at the photosphere at these phases. The inset is a zoom of the region around the 6320 Å notch in the −7 day spectrum.

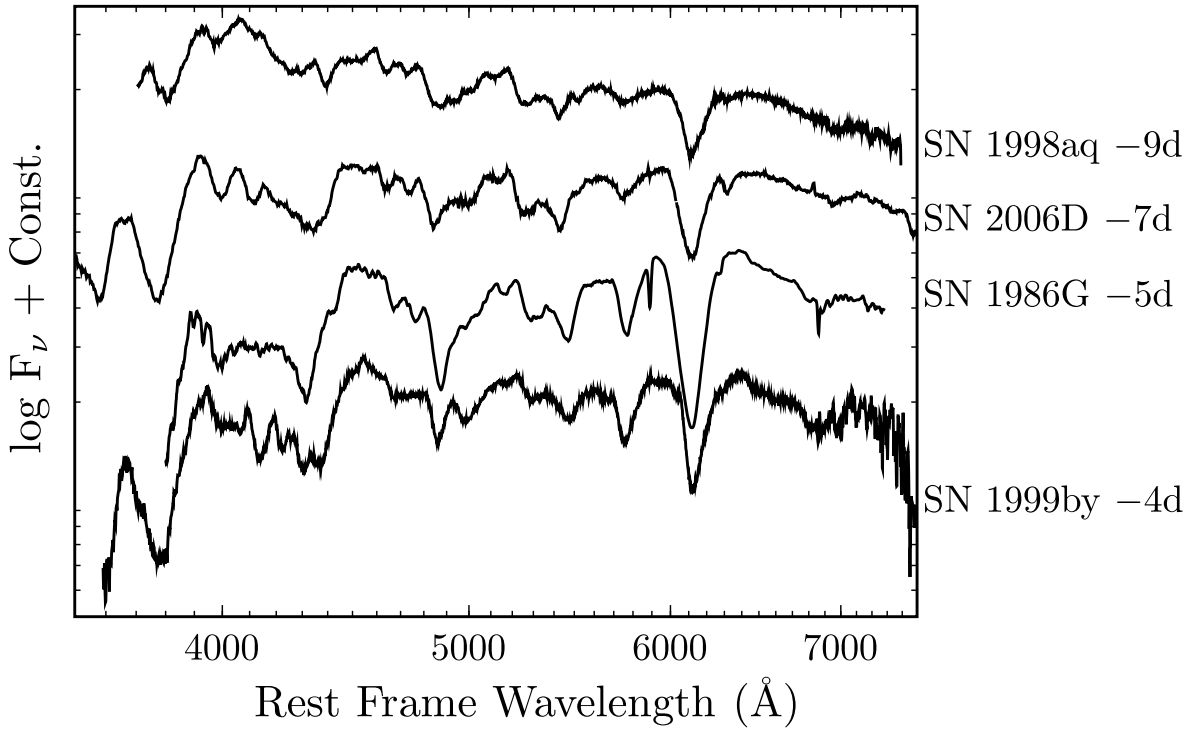

Fig. 2.— Comparison of the −7 day spectrum of SN 2006D to premaximum spectra of SNe 1998aq, 1986G, and 1999by.

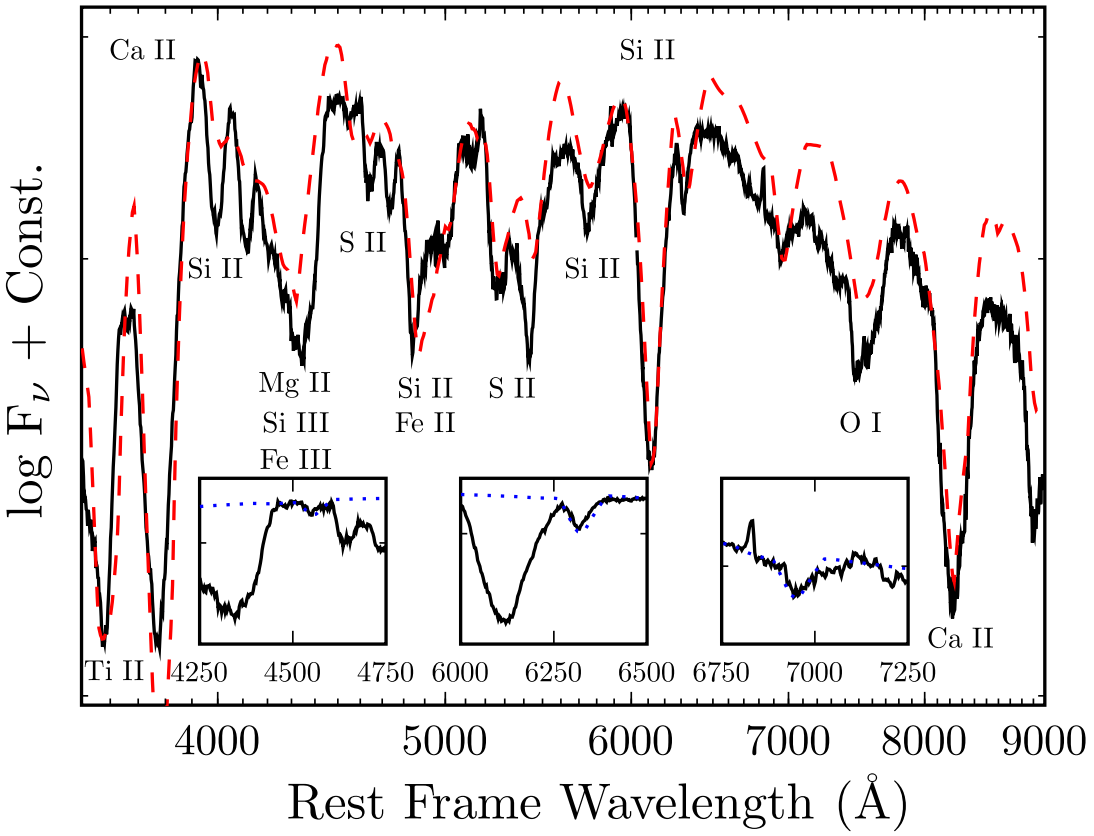

Fig. 3.— Synthetic spectra overlaid on the −7 day spectrum of SN 2006D. Inset plots show the coincidence between the synthetic C II spectrum and the data.

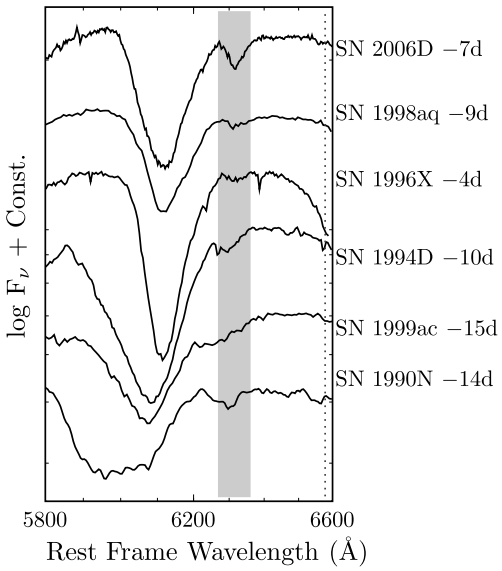

Fig. 4.— Comparison of C II λ6580 feature across several premaximum SN Ia spectra. The spectra are resampled into 10 Å bins.